

A silicon UCN detector with large area and
with analysis of UCN polarization

M. Lasakov¹, A. Serebrov¹, A. Khusainov¹,
A. Pustovoi¹, Yu. Borisov¹, A. Fomin¹,
P. Geltenbort², O. Kon'kov³, I. Kotina¹,
A. Shablii¹, V. Solovei¹, A. Vasiliev¹

¹ *St. Petersburg Nuclear Physics Institute, Gatchina, Russia*

² *Institut Max von Laue – Paul Langevin, Grenoble, France*

³ *Ioffe Physical Technical Institute, St.Petersburg, Russia*

Corresponding author: A.P. Serebrov

A.P. Serebrov

Petersburg Nuclear Physics Institute

Gatchina, Leningrad district

188300 Russia

Telephone: +7 81271 46001

Fax: +7 81271 30072

E-mail: serebrov@pnpi.spb.ru

Abstract

A silicon UCN detector with an area of 45 cm^2 and with a ${}^6\text{LiF}$ converter is developed at PNPI. The spectral efficiency of the silicon UCN detector was measured by means of a gravitational spectrometer at ILL. The sandwich-type detector from two silicon plates with a ${}^6\text{LiF}$ converter placed between them was also studied. Using this type of technology the UCN detector with analysis of polarization was developed and tested. The analyzing power of this detector assembly reaches up 75% for the main part of UCN spectrum. This UCN detector with analysis of UCN polarization can be used in the new EDM spectrometer.

PACS: 28.20.-v

Keywords: Ultracold neutrons

Introduction

Ultracold neutrons (UCN) have been actively used in basic research since the beginning of the 70-s. The property of UCN to be reflected from the matter at any incidence angles allows to store them in material traps. It opens up possibilities to measure neutron lifetime [1], to measure electric dipole moment of neutron [2] and to carry out other experiments, using this outstanding property of UCN.

The most common method of UCN detection is based on using a gaseous proportional counter containing small admixture of ^3He gas within an argon atmosphere [3]. This detector has Al foil as its window. It cuts down efficiency of UCN registration especially in the region of low energies because boundary velocity of UCN reflection from Al is 53 neV. This disadvantage can be compensated if we use this detector with a vertical guide about 1 m height to accelerate UCN in the gravitational field.

Another type of UCN detector was developed in recent years [4,5,6]. It is based on usage of a silicon diode with a ^6Li converter coated on its surface ($n + ^6\text{Li} \rightarrow \alpha$ (2.65 MeV) + ^3H (2.73 MeV)). Li is usually used as LiF compound due to its chemical activity. ^6Li has an absorption cross section for thermal neutrons of 945 barn. LiF (95% ^6Li) thickness of 0.6 mg/cm^2 is sufficient to obtain absorption efficiency of 95% for UCN with a velocity of 10 m/s. α -particle ($E=2.05 \text{ MeV}$) has a path of 1.5 mg/cm^2 , triton ($E=2.73 \text{ MeV}$) has a path of 7.4 mg/cm^2 . It was shown that LiF (95% ^6Li) thickness of 0.6 mg/cm^2 allows to have the maximum efficiency of UCN registration [4].

The boundary velocity of LiF (95% ^6Li) is 125 neV, but it is necessary to mention that the density of coated LiF is 30% less than its theoretical density in the crystal

[7]. The compounds of LiF and Ti or LiF and ^{62}Ni are used to decrease the boundary velocity of the converter [8,6]. But it decreases the efficiency of α -particles leaving the converter. The thickness of the converter can be reduced twice as much using a ^{58}Ni ($E_{\text{boundary}} = 330 \text{ neV}$) coating on the surface of Si detector. In this case the part of UCN not absorbed in the converter is reflected from the ^{58}Ni and is absorbed almost completely while going through the converter for the second time [6]. The main advantages of the Si detector in comparison with the gaseous proportional detector are that it can be installed directly into vacuum and that it can be used at low temperatures down to the temperature of liquid helium. However, the Si UCN detector has a small square of about $3\div 4 \text{ cm}^2$ and due to this it gives way to the gaseous proportional UCN detector in practice.

The aims of this work were: 1) development of a Si UCN detector with a large square of $\sim 50 \text{ cm}^2$; 2) measurement of its spectral efficiency; 3) research with the Si UCN detector from two Si plates and a ^6LiF converter between; 4) development of a detector with polarization analysis and measurement of its analyzing power.

The experimental setup

The PNPI gravitational spectrometer was used for measurements of the spectral efficiency of the detector. This experiment was carried out at the UCN source of the high intensity ILL reactor [9]. The scheme of the experimental setup is presented in the Fig. 1. It consists of a gravitational spectrometer, a superconducting solenoid for polarizing of UCN, a neutron guide system and detectors. The neutron guide system was able

to rotate around the axis of the horizontal neutron guide and, thus, the detector position had different height relative to the horizontal neutron guide. It allowed us to change UCN energy due to acceleration in the gravitational field and to study spectral efficiency of the detector. In the studies of spectral analyzing power of the special detector with the polarization analysis the superconducting solenoid was used, which polarized UCN. The magnetic field of the superconducting solenoid produces a potential barrier for one spin component of the neutron beam and a potential well for the other one. The magnetic field of 4.5 T produces conditions when only one spin component goes through the solenoid, the other component with the energy less than 270 neV is reflected. Al foil or Si wafer were placed in the horizontal neutron guide instead of the unit for rotation to measure energy dependence of UCN transmission for energies of 20-180 neV, the UCN detector was placed in the low position, i.e. 1 m lower than the horizontal neutron guide. The foils were placed in front of the detector being in the down position to measure this transmission dependence for UCN energies up to 300 neV.

Measurement of the energy dependence of UCN transmission through Al foils and a Si wafer

The gravitational spectrometer was used for a measurement of the energy dependence of UCN transmission. UCN from the turbine filled the cylindrical trap of the gravitational spectrometer (\varnothing 490 mm, $h = 2200$ mm). After closing the shutters UCN were held for 10 s to prepare a spectrum of neutrons with a given maximum energy. Neutrons with kinetic energy higher than the corresponding absorber position were lost

during this time. Then the shutter 2 was opened and neutrons passing the neutron guide system were registered by the UCN detector in the low position (II). Time of registering was 100 s and time of emptying of the spectrometer trap was 40 s. This operation was repeated with different absorber positions. Different count rates for different absorber positions allow to obtain the spectrum of UCN stored in the trap if the detection efficiency is energy independent. Otherwise the product of UCN spectrum and energy dependent detector efficiency is measured.

These measurements were repeated with an Al foil (100 μm) or a Si wafer (375 μm) placed in the neutron guide. The UCN transmission coefficient through a foil is the ratio of detector count rates with the foil and without it. Fig. 2 shows UCN transmission coefficients measured for energies of 60-300 neV. For measurements with low energies the foils were placed in the horizontal part of the neutron guide, for measurements with high energy foils were placed in front of the detector being in the down position.

This method takes into account multiple interactions of UCN with the foil, the trap and the detector and gives adequate information for work with UCN when they are registered after storage in traps. The Si wafer has a better transmission coefficient although it is considerably thicker. This is because the Si monocrystal has a more homogeneous density as compared to the rolled unannealed Al foil. The obtained result allows to make conclusions about the possibility to develop Si detectors of a sandwich type which use a converter of UCN into charged particles between two Si detectors. Its advantage is a 4π -geometry for registration of tritons that are not absorbed in the converter due to their big track length. Probably, the efficiency of UCN registration by this

detector can be the same as energy dependence of transmission through Si wafer. Thus, it can be somewhat better or equal to the efficiency of ^3He detector.

A Si UCN detector with large area and measurement of its energy dependent efficiency

For the production of the Si UCN detector with large area we used a Si wafer of 78 mm diameter. The area of the detector (48 cm^2) was divided into four parts to decrease the capacity of the detector. It allows to keep the amplitude of the signal at a sufficiently high level with respect to detector noise. The detector with single Si wafer is shown in the Fig. 3.

The surface of the detector was coated by ^6LiF (^6Li 80%) with a thickness of $0.6\text{-}0.8\text{ mg/cm}^2$. The energy dependence of the registration efficiency was measured using the gravitational spectrometer. For that the spectrum of the registered UCN was measured in the detector position I at the level of the horizontal guide ($h_d=0$) and in the detector position II (down) ($h_d=1\text{ m}$). The ratio of these spectra can be considered as the registration efficiency of the detector at the level of the horizontal guide if we suppose that the registration efficiency in the down position is 100% due to the gravitational acceleration. A correction to this assumption can be obtained from the energy dependence of the spectral ratio and from measurements in the intermediate positions between $h_d=0$ and $h_d=1\text{ m}$. The spectrum of the registered neutrons was measured in the down position in order to compare the registration efficiencies of the Si detector and the ^3He detector. It allowed to compare the detector efficiency for the upper part of the energy spectrum.

The total count rate for the Si detector was 5% higher than for the ^3He detector. The transmission coefficient through the Al window (100 μm) of the ^3He UCN detector was taken as its absolute registration efficiency. Fig. 4 presents the energy dependence of the registration efficiency for the ^3He UCN detector with an Al window (100 μm) and for the Si detector with a single ^6LiF (80% ^6Li) converter on its surface. Efficiencies of both detectors were compared in the upper part of the spectrum when detectors were in the down position.

The efficiency of the Si detector is better than that of the ^3He detector although the boundary velocity of ^6LiF (80% ^6Li) is higher than the boundary velocity of the ^3He detector Al window. It is connected with that the absorption coefficient of materials with a high capture cross section is sufficiently bigger for the region of low energies and that the density of coated ^6LiF is 30% lower than the density of a LiF crystal [7].

A Si sandwich UCN detector with two Si wafers and a ^6LiF converter

This detector was developed at PNPI and investigated in an experiment at ILL. It allowed to obtain the fraction of α -particles lost in the ^6LiF converter by signal summation from the first and the second detectors and application of coincidence and anti-coincidence techniques. Fig. 5 shows spectra of signals from the first and the second detectors, the spectrum of sum of signals from both detectors and the spectrum of sum of signals from both detectors but without coincidence between them. The fraction of signals without coincidence is about 28% and corresponds to events for which the triton

was registered and the α -particle was absorbed in the ${}^6\text{LiF}$ converter. The thickness of the converter was $0,6-0,8 \text{ mg/cm}^2$.

The results of the measurements allow us to conclude that the detector with one Si wafer and ${}^6\text{LiF}$ converter loses 14% of events due to α -particle absorption in the ${}^6\text{LiF}$ converter. Thus, the registration efficiency of this detector is about 86%. This conclusion does not contradict with the results of registration efficiency measurements carried out with the gravitational spectrometer.

The Si sandwich UCN detector is fully efficient for tritons, but decreases the flux of falling UCN with energies of 200-300 neV by about 20-25%. Thus, the Si sandwich detector has 75-80% efficiency for UCN with energies of 200-300 neV. It should be used with a vertical guide to accelerate UCN in the gravitational field, like the ${}^3\text{He}$ detector with an Al window.

A Si UCN detector with polarization analysis

The scheme of this detector is presented in the Fig. 6. The detector consists of an upper detector for registration of “up” spin component and a down detector for registration of “down” spin component. “Up” and “down” polarization components are defined in compliance with the position of the neutron energy levels in the magnetic field. A magnetized ferromagnetic film is placed between the detectors which reflects the “up” spin component and allows the “down” spin component to pass. The down detector is a mosaic of five single detectors $2 \times 6 \text{ cm}^2$. The upper detector consists of four single detectors $2 \times 6 \text{ cm}^2$ grouped around the neutron guide. The area of the upper detector is

20% less than the area of the down detector and a part of the reflected neutrons returns to the neutron guide. But they have a chance to return and to be analyzed again.

The analyzing power of the detector can be defined by the polarizing ratio:

$$R = \frac{N_d - N_{up}}{N_d + N_{up}} = P \cdot A, \quad (1)$$

where N_{up} - count rate of the upper detector, N_d - count rate of the down detector, P - UCN polarization, A - analyzing power. In the ideal case this ratio is equal to 1 when the flux is completely polarized (solenoid is switched on) and it is equal to 0 when the flux is unpolarized (solenoid is switched off). In reality there are several circumstances which disturb these correlations: the registration efficiencies of the detectors are different because of different areas; there is an effect of reflection of UCN from materials which does not depend on polarization of neutrons and decreases efficiency of polarization analysis; and the analyzing power of the detector depends on the properties of the analyzing ferromagnetic foil. Different materials which could be used as a substrate for thin ferromagnetic films were studied: Al foils (annealed and unannealed) and Si wafers.

The main requirement for a substrate is to be transparent for UCN. Moreover, the surface of the substrate should be like a mirror and parallel to the magnetic field direction. Fig.7 presents reflection and transmission coefficients for Al foils and Si wafer. The bottom abscissa axis shows UCN energy on the foil and the top abscissa axis shows UCN energy in the horizontal neutron guide (it is 100 neV less). The left ordinate axis shows the ratio of upper and down detector count rates, which describes a reflection coefficient of UCN from the foil. The right ordinate axis shows the ratio of the down de-

tector counts with the foil and without it, which describes the transmission coefficient of UCN through the foil. It is possible to see that the Si detector itself is the most suitable substrate. But we were not able to prepare a Si detector coated with ferromagnetic film. So we used an analyzer which was a pure iron film of natural isotope composition with thickness of 1500-2000 Å coated onto annealed Al foil (90 μm). It was kindly placed at our disposal by the group from Sussex University which uses these analyzers (polarizers) in their nEDM experiment.

Fig. 8 shows energy dependence of polarizing ratio (1) for flux with full polarization (solenoid is switched on, $H=4T$) and for unpolarized flux (solenoid is switched off, $H=0T$). When we change the UCN polarization from 1 to 0, the polarizing ratio is changed by 0.8. Overall this result is not bad. The imperfection in splitting of spin components is connected with an effect of UCN reflection from the detector and the substrate of the analyzer. Measurements of the detector count rate ratios with Al substrate but without ferromagnetic film showed that the albedo effect is determinative. Using the ratio obtained in these measurements as a correction allows to reconstruct almost completely the full polarization value. The empty squares and circles are polarization ratios for polarized and unpolarized flux after correcting for the albedo effect. As a first approximation the correction for polarized flux is $2r$ and for unpolarized flux is $r/2$, where r is a detector count rate ratio with similar conditions but without ferromagnetic film. So, it is reasonable to use a Si detector as a substrate for the analyzer and to decrease the boundary velocity of the converter if we want to obtain a better efficiency of the analyzing system. Using a compound (LiFTi) can decrease the boundary velocity of the con-

verter. Increasing the converter thickness is not a problem because a detector of sandwich type registers tritons, which have a sufficiently long free path, in 4π -geometry.

In conclusion, the newly developed UCN detector with polarization analysis is very promising, e.g. for an application in the nEDM experiment. Obtained parameters of this detector are sufficient to solve the task, but further improvements are expedient. The authors are grateful to: K. Kirch and O. Naviliat for useful discussions, Paul Scherrer Institute for the financial support of this work as well as the Russian Foundation of Basic Research for the support under the contracts 02-02-17120 and 04-02-17440, INTAS for the support under the contract 2001-765, the Russian Academy of Science for the support under the Program of Fundamental Research.

References

- [1] Zeldovich Ya.B. *Sov. Phys. JETP* 9: 1389 (1959)
- [2] Shapiro F.L. 1968 *Sov. Phys. Usp.* 11 345
- [3] Groshev L.V. et al., *Proceedings All-Union Conference on Neutron Physics*, part 4, p.264 (1974) (in Russian)
Ignatovich V.K., *The Physics of Ultracold Neutrons*, Oxford: Clarendon, p.62 (1990) (in English)
- [4] Baker C.A. et al., *NIM A*487 (2002) 511-520
- [5] Kitagaki T. et al., *Proceedings of the 15th International Collaboration on Advanced Neutron Sources* (Tsukuba, Japan) (2000)
- [6] Maier-Komor P. et al., *NIM A*480 (2002) 109-113

[7] Bates J.C. NIM 150 (1978) 261-272

[8] Kawai T. et al., NIM A378 (1996) 561-563

[9] Steyerl A. et al., 1986 *Phys. Lett.* 116A 347-52

Fig. 1. The scheme of the experimental setup for measurements of spectral efficiency of detectors and spectral efficiency of polarization analysis.

Fig. 2. Transmissions through the Al foil (100 μm) and the Si wafer (375 μm).

-□- 375 μm (wafer is in the horizontal guide);

-■- Si 375 μm (wafer is in front of the detector being in down position);

-Δ- Al 100 μm (foil is in horizontal guide);

-▲- Al 100 μm (foil is in front of the detector being in down position).

Fig. 3. A four fold segmented, 3 inch Si UCN detector.

Fig. 4. Energy dependence of registration efficiency: -■- ^3He UCN detector with Al window (100 μm); -▲- Si detector with ^6LiF (80% ^6LiF) converter on its surface.

Fig. 5. Spectrum of signals: a) first detector, b) second detector, c) sum of signals from both detectors, d) sum of signals from both detectors but without coincidence between them.

Fig. 6. Scheme of Si UCN detector with polarization analysis.

Fig. 7. Reflection and transmission coefficients for Al foils and Si wafer: -◆- is a reflection coefficient for Si wafer 350 μm ; -Δ- are reflection and transmission coefficients for annealed Al foil 90 μm ; -○- are reflection and transmission coefficients for unannealed

Al foil 15 μm ; $-\square-$ are reflection and transmission coefficients for unannealed Al foil 100 μm .

Fig. 8. Energy dependence of polarizing ratio: $-\blacksquare-$ are for flux with full polarization (solenoid is switched on, $H=4\text{T}$); $-\bullet-$ are for unpolarized flux (solenoid is switched off, $H=0\text{T}$). $-\square-$ and $-\circ-$ correspond to the values corrected for the albedo effect.

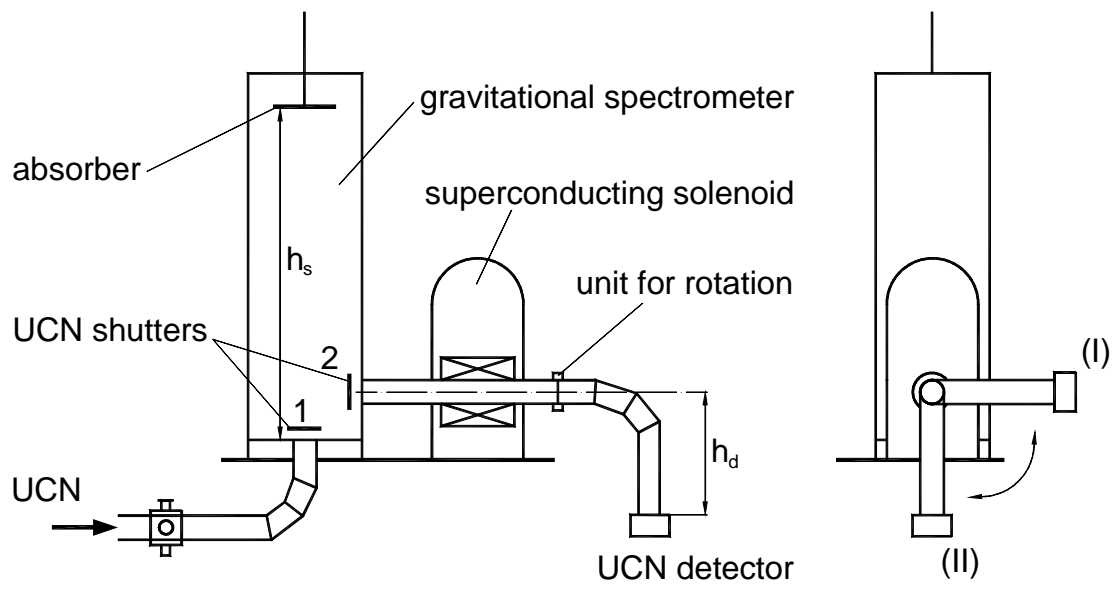


Fig. 1.

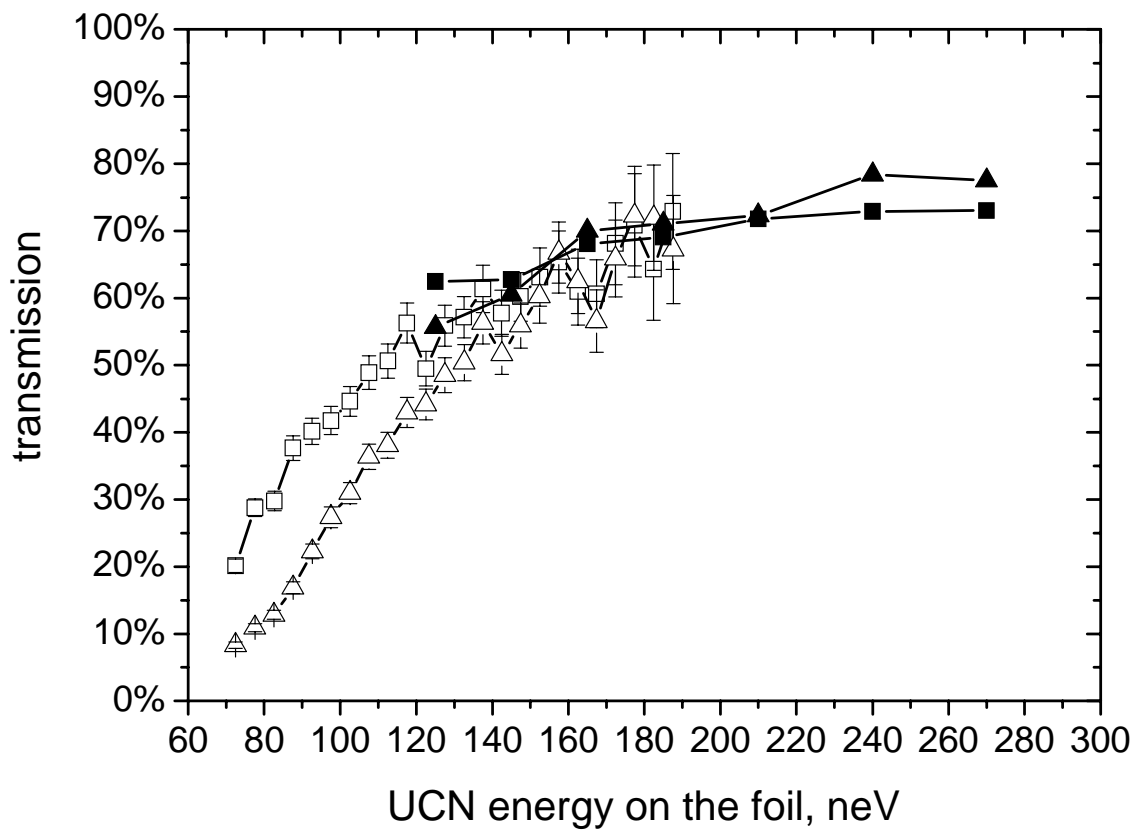


Fig. 2.

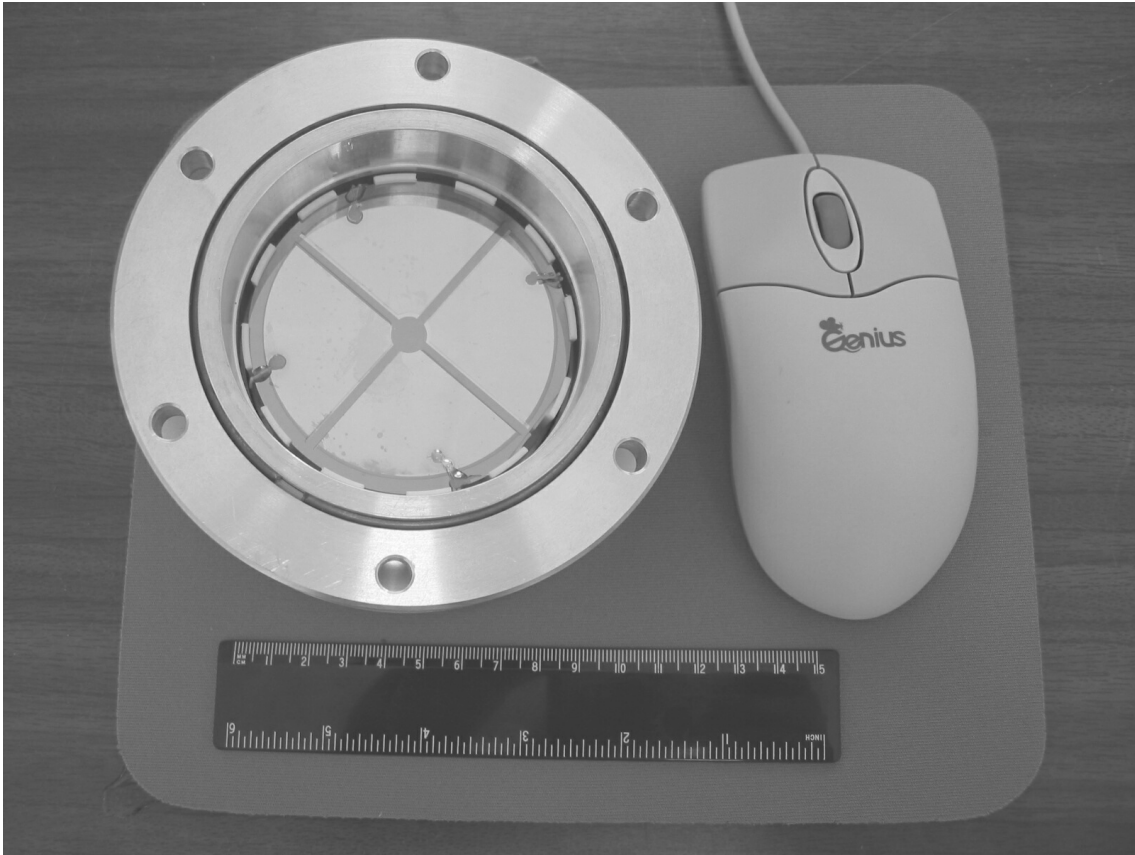


Fig. 3.

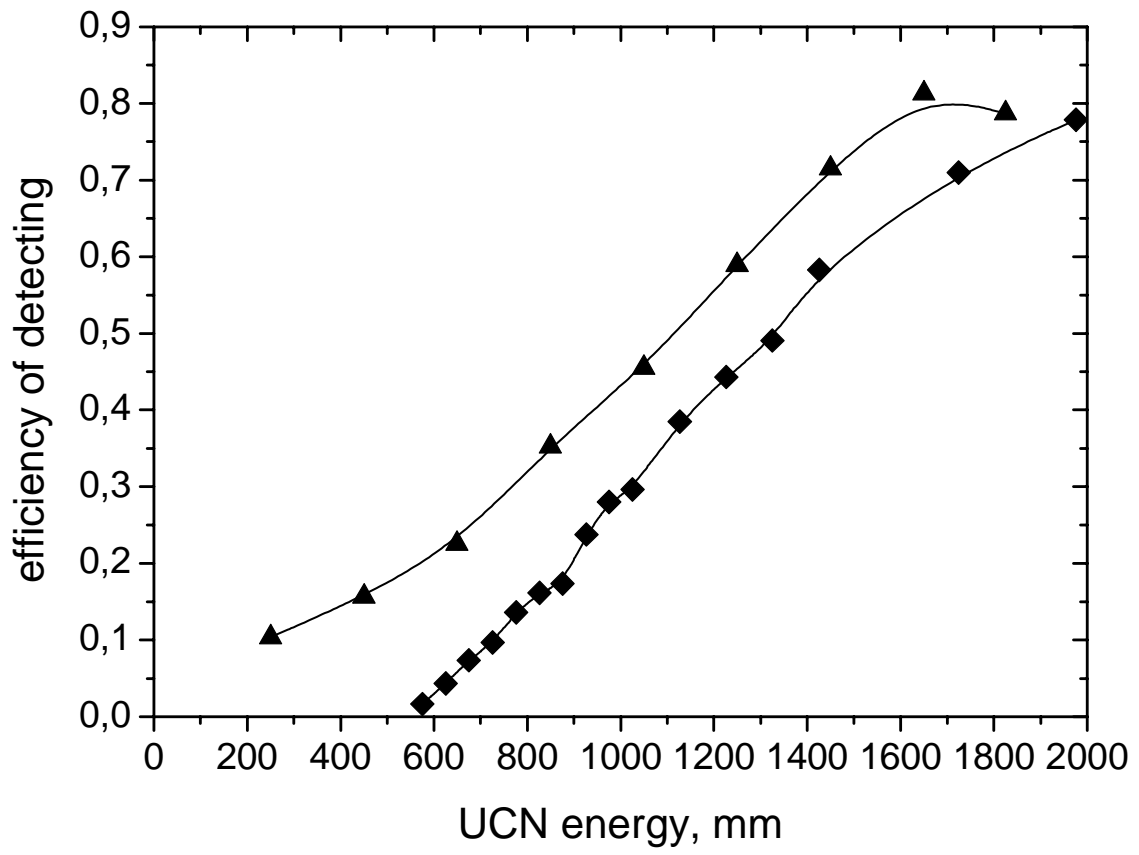


Fig. 4.

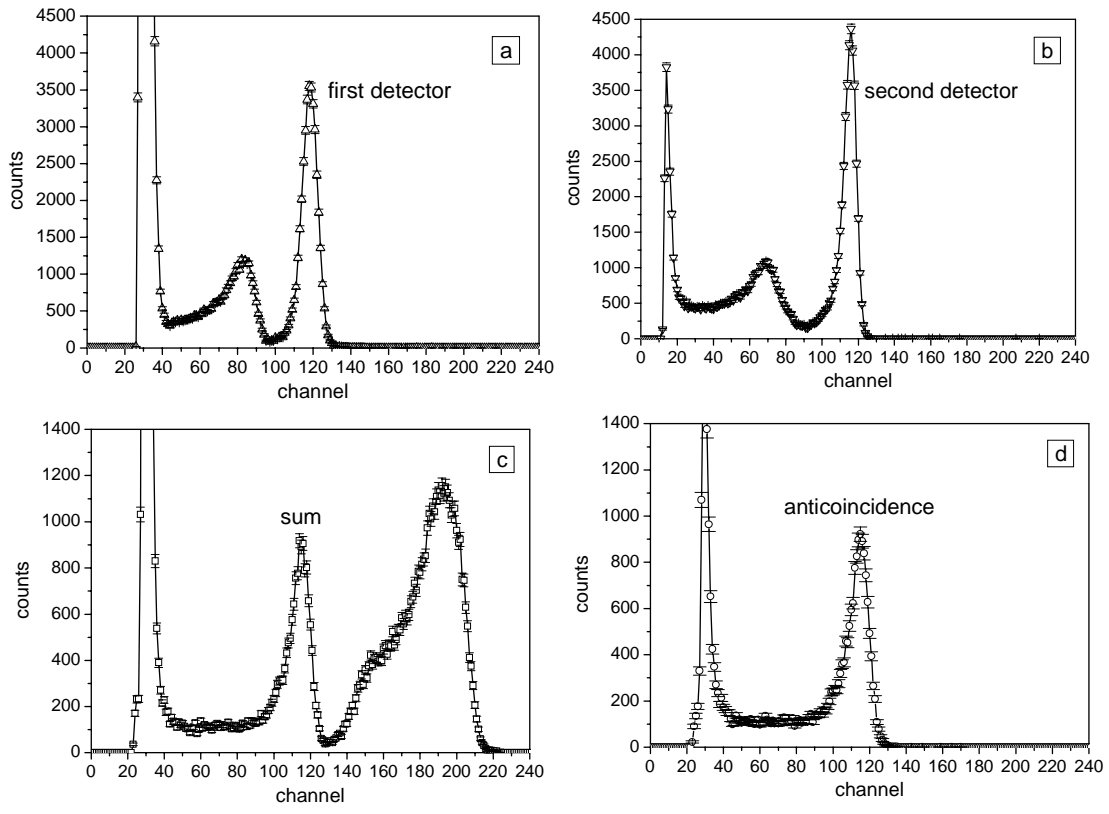


Fig. 5.

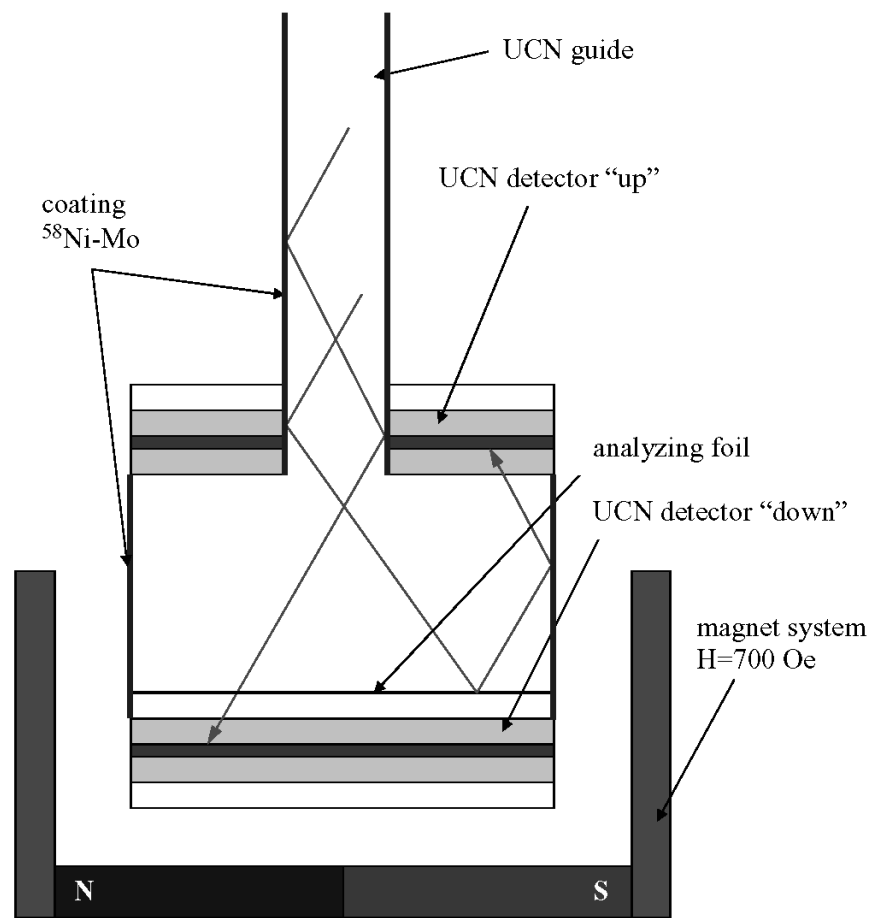


Fig. 6.

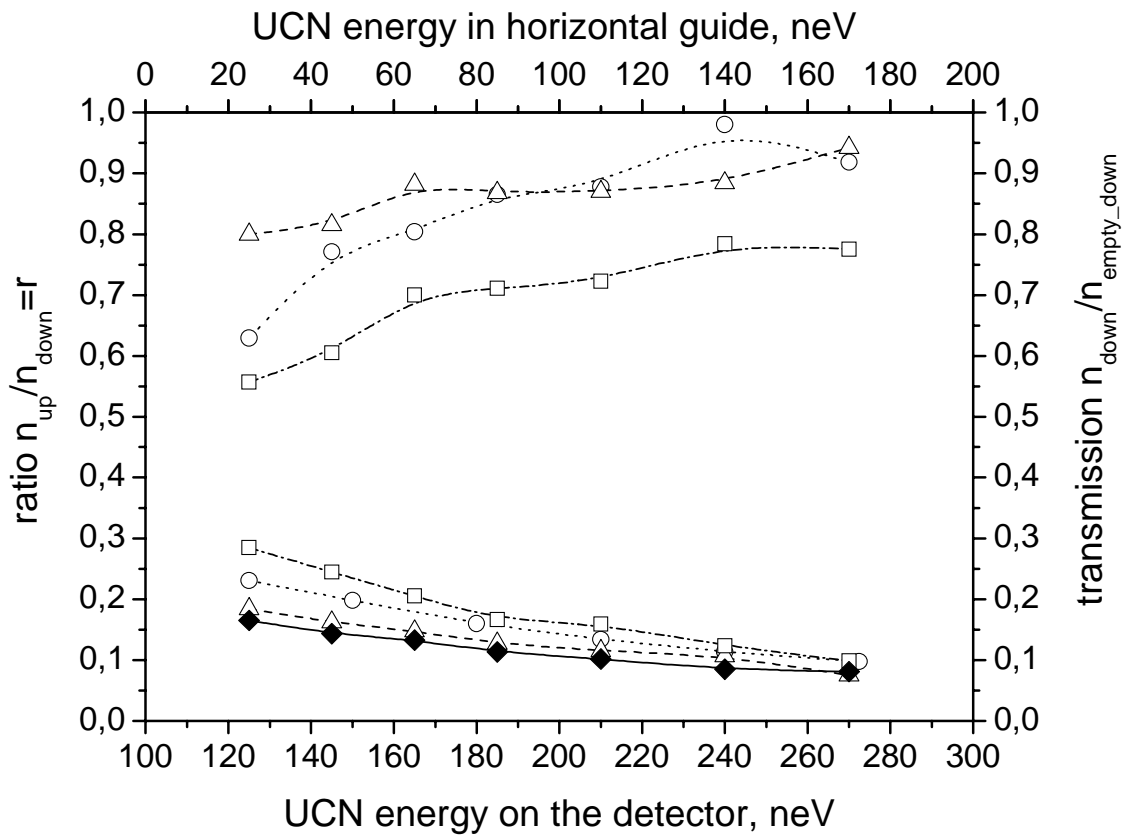


Fig. 7.

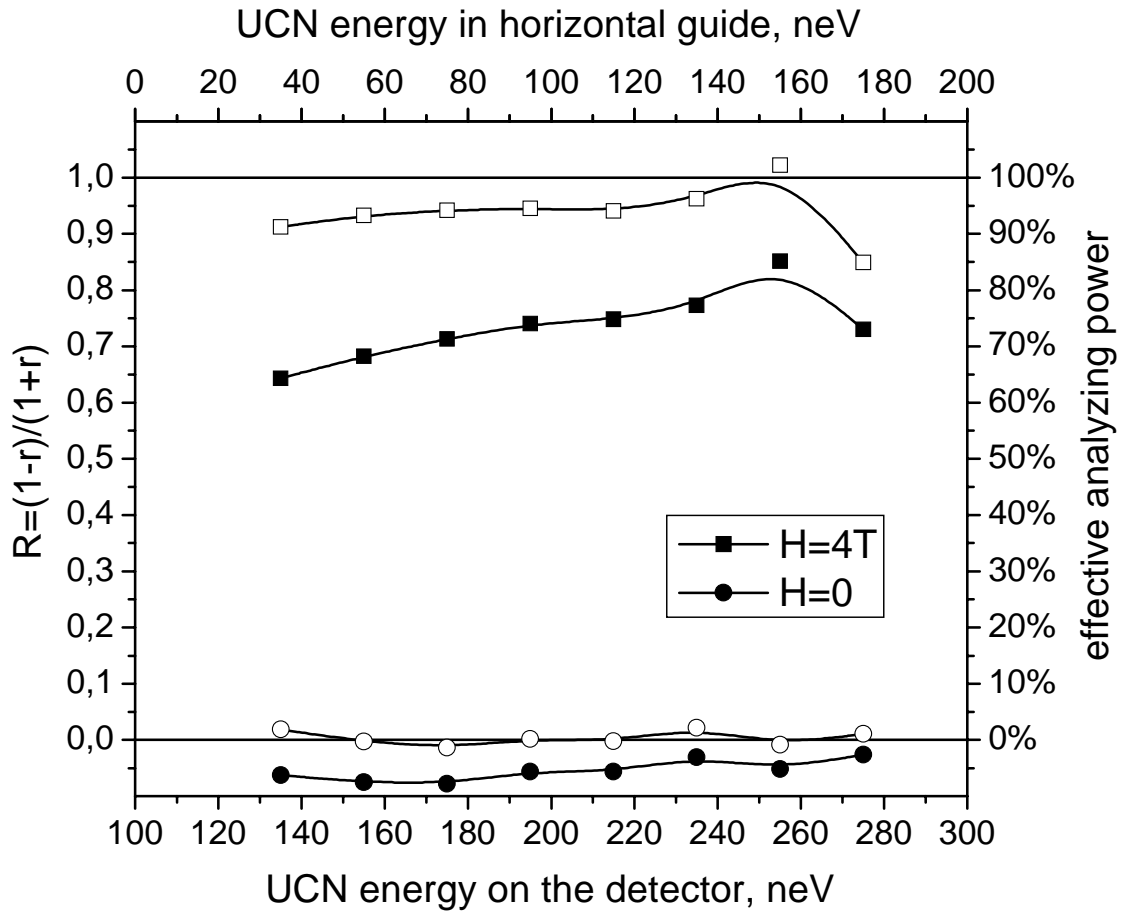


Fig. 8.